Published for SISSA by Springer

Received: *September 26, 2013*
Revised: *December 17, 2013*
Accepted: *January 20, 2014*
Published: *February 10, 2014*

Higgs phenomenology in the two-singlet model

Amine Ahriche,[a] **Abdesslam Arhrib**[b,c] **and Salah Nasri**[d]

[a] *Department of Physics, University of Jijel, PB 98 Ouled Aissa, DZ-18000 Jijel, Algeria*
[b] *Département de Mathématiques, Faculté des Sciences et Techniques, Université Abdelmalek Essaadi, B. 416, Tangier, Morocco*
[c] *Institute of Physics, Academia Sinica, Nankang, Taipei 11529, Taiwan*
[d] *Department of Physics, UAE University, P.O. Box 17551, Al-Ain, United Arab Emirates*

E-mail: aahriche@ictp.it, aarhrib@ictp.it, snasri@uaeu.ae.ac

Abstract: We study the phenomenology of the Standard Model (SM) Higgs sector extended by two singlet scalars. The model predicts two CP-even scalars $h_{1,2}$ which are a mixture of doublet and singlet components as well as a pure singlet scalar S_0 which is a dark matter candidate. We show that the model can satisfy the relic density and direct detection constraints as well as all the recent ATLAS and CMS measurements. We also discuss the effect of the extra Higgs bosons on the different Higgs triple couplings $h_i h_j h_k$, $i, j, k = 1, 2$. A particular attention is given to the triple self-coupling of the SM-like Higgs where we found that the one loop corrections can reach 150% is some cases. We also discuss some production mechanisms for h_1 and h_2 at the LHC as well as at the future International Linear Collider. It is found that the production cross section of a pair of SM-like Higgs bosons could be much larger than the corresponding one in the SM and would reveal physics beyond the SM if observable. We also show that in this model the branching ratio of the SM-like Higgs decaying to two singlet scalars could be of the order of 20%, therefore the production of the SM Higgs followed by its decay to a pair of singlets would be an important source of production of singlet scalars.

Keywords: Higgs Physics, Beyond Standard Model, Cosmology of Theories beyond the SM

ArXiv ePrint: 1309.5615

doi:10.1007/JHEP02(2014)042

JHEP02(2014)042

Contents

JHEP02(2014)042

1 Introduction

The Large Hadron Collider (LHC) at CERN has just successfully finished its first phase of operation with a 7 and 8 TeV run. Both experiments ATLAS and CMS at the LHC announced last July the discovery of a Higgs-like particle with a mass in the range 125–126 GeV [1, 2]. Both collaborations, ATLAS and CMS reported a clear excess in the two photon channel and in the ZZ^* channel [1, 2]. The discovery is also confirmed with less significance in other channels [3–6], like WW^* which has a lower mass resolution, and also by the final Tevatron results reported by CDF and D0 experiments [7].

The extraction of the couplings of the Higgs-like particle to gauge bosons and fermions achieved up to now from the $7 \oplus 8$ TeV data shows that this particle looks more and more like the SM Higgs boson [3–6], while more data is needed in order to fully pin down the exact nature of the newly discovered particle.

Although, ATLAS and CMS data show no significant deviation of the signal from the SM predictions. At ATLAS, the diphoton channel shows some small enhancement. The overall signal strength for diphoton is about $1.55^{+0.33}_{-0.28}$, which corresponds to about 2 σ deviation from the SM prediction [8]; while the other channels are consistent with the SM. However, at CMS, the new analysis for diphoton mode based on multivariate analysis [9] gives 0.77 ± 0.27, which is compatible with the SM. Many models beyond the SM have been

proposed to explain the diphoton excess, but the actual disagreement between ATLAS and CMS does not allow to extract significant conclusions.

Since the Higgs-like particle decays to two photons, it can not be spin one particle because of the Young Landau theorem, it is either spin-0 or spin-2. Recently, spin and parity of the Higgs-like particle were studied from the angular distribution of the diphoton, ZZ^* and WW^* decay channels [10–13] at ATLAS and CMS. Both collaborations disfavor the pure pseudoscalar hypothesis $J^P = 0^-$; and also a pure spin-2 hypothesis. In addition, the spin one hypotheses is also disfavored with an even higher confidence.

Therefore, the first phase of the LHC run is just the beginning of a precise measurement program that starts with $7 \oplus 8\,\text{TeV}$ data and will be completed with the second run of the LHC at 13–14 TeV as well as by the International Linear Collider (ILC). It is well known that the precise measurement programs at the ILC and the LHC are complementary [14, 15]. Such measurements, if accurate enough, can be also helpful in discriminating between models through their sensitivity to radiative correction effects, in particular in specific cases like the decoupling limit. It is well known that many SM extensions such as SUSY models or extended Higgs sector models possess such decoupling limit where the light Higgs boson completely mimics the SM Higgs.

ATLAS and CMS discovery, has lead to several phenomenological constraints on the scalar sector in such extensions of SM Higgs sector with extra doublets, Higgs sector with doublet and singlets, or Higgs sector with doublet and triplets etc... The fact that the Higgs-like particle couplings to gauge bosons and fermions are consistent with the SM predictions; can put severe constraints on all beyond SM extensions that try to accommodate such Higgs-like particle.

The aim of this paper is to study the phenomenology of the SM Higgs sector extended by two real, spinless and $\mathbb{Z}_2$ symmetric fields which can explain the Dark Matter (DM) [16–19]. The model has three CP-even scalars, two of which, $h_{1,2}$, are mixing of a $\text{SU}(2)_L$ doublet and a singlet, whereas a $\mathbb{Z}_2$-odd singlet S_0 remains unmixed, which can play the role of DM candidate. However, both h_1 and h_2 can decay to a pair of S_0, if kinematically allowed, it will contribute to the invisible decay of h_1 or h_2; and will potentially modify the properties of the Higgs-like particle h_1 or h_2. In addition, the annihilation of S_0 into SM particles will provide thermal relic density and the scattering of S_0 on nucleons will lead to direct detection signatures.

In the light of the recent discovery of a 125 GeV Higgs-like particle [1, 2], we investigate, in the framework of the two singlets model, the possibility that one of the scalars h_1 or h_2 is the particle observed by ATLAS and CMS. Therefore, we consider the two cases where one of the scalar eigenmasses m_1 or m_2 lies in the range 123.5–127.5 GeV tolerated by ATLAS and CMS experimental results, with their couplings to the SM fermions and gauge bosons close to the SM case, i.e., $g^2_{h_i f\bar{f}}/g^{2(\text{SM})}_{hf\bar{f}} = g^2_{h_i VV}/g^{2(\text{SM})}_{hVV} \geq 0.9$. Then, we will investigate the phenomenology of the non SM-like Higgs in both cases.

This paper is organized as follows. We first introduce the two singlet model and its theoretical constraints in the second section. We investigate the DM and its direct detection constraints on the two singlet model in the third section. Section 4 is devoted to various Higgs triple self-couplings that exist in this model with particular attention given

JHEP02(2014)042

to the triple self-coupling of the SM-like Higgs scalar. We discuss some phenomenological aspects of the model such as the Higgs decays and double Higgs production in section V and present our conclusion in section 6. In the appendices, we give the tree-level cubic and quartic scalar couplings and we provide the details of the calculation of the effective Higgs triple couplings from the effective potential.

2 The two-singlet model

In this model, we extend the Standard Model with two real scalar fields S_0 and χ_1; which transform under the discrete symmetry $\mathbb{Z}_2^{(0)} \otimes \mathbb{Z}_2^{(1)}$ as

$$\begin{aligned} \mathbb{Z}_2^{(0)}: &\quad (S_0, \chi_1) \to (-S_0, \chi_1) \\ \mathbb{Z}_2^{(1)}: &\quad (S_0, \chi_1) \to (S_0, -\chi_1). \end{aligned} \tag{2.1}$$

The field χ_1 has a non vanishing vacuum expectation value, which breaks $\mathbb{Z}_2^{(1)}$ spontaneously, whereas, $\langle S_0 \rangle = 0$; and hence, S_0 is a dark matter candidate. Both fields are standard model gauge singlets and hence can interact with 'visible' particles only via the Higgs doublet H. The part of the Lagrangian that includes the fields S_0, H, and χ_1 is written as follows:

$$\mathcal{L} = (D_\mu H)^\dagger D_\mu H + \frac{1}{2}(\partial_\mu S_0) + \frac{1}{2}(\partial_\mu \chi_1) - V(H, \chi_1, S_0), \tag{2.2}$$

with

$$\begin{aligned} H^T &= \left(h^+, \quad (\upsilon + \widetilde{h} + i\chi_0)/\sqrt{2}\right), \; D_\mu H = \left(\partial_\mu - ig_2/2\sigma^a W_\mu^a - ig_1/2B_\mu\right) H, \\ \chi_1 &= \upsilon_1 + \widetilde{\chi}_1, \end{aligned} \tag{2.3}$$

where σ^a are the Pauli matrices, W_μ^a (B_μ) and g_2 (g_1) are the $\mathrm{SU}(2)_L$ ($\mathrm{U}(1)_Y$) gauge field and coupling, respectively. The tree-level scalar potential that respects the $\mathbb{Z}_2$ symmetries is given by [16–18]

$$\begin{aligned} V(H, \chi_1, S_0) = &-\mu^2 H^\dagger H + \frac{\lambda}{6}\left(H^\dagger H\right)^2 + \frac{\widetilde{m}_0^2}{2} S_0^2 - \frac{\mu_1^2}{2}\chi_1^2 + \frac{\eta_0}{24} S_0^4 + \frac{\eta_1}{24}\chi_1^4 \\ &+ \frac{\lambda_0}{2} S_0^2 H^\dagger H + \frac{\lambda_1}{2}\chi_1^2 H^\dagger H + \frac{\eta_{01}}{4} S_0^2 \chi_1^2. \end{aligned} \tag{2.4}$$

The parameters μ^2 and μ_1^2 could be eliminated from the potential by imposing (υ, υ_1) to be the absolute minimum as

$$\begin{aligned} \mu^2 &= \lambda\upsilon^2/6 + \lambda_1\upsilon_1^2/2 + \frac{1}{\upsilon}\frac{\partial}{\partial\widetilde{h}} V^{1-l}\Big|_{\tilde{h}=\upsilon, \chi_1=\upsilon_1, S_0=0.}, \\ \mu_1^2 &= \eta_1\upsilon_1^2/6 + \lambda_1\upsilon^2/2 + \frac{1}{\upsilon_1}\frac{\partial}{\partial\chi_1} V^{1-l}\Big|_{\tilde{h}=\upsilon, \chi_1=\upsilon_1, S_0=0.}, \end{aligned} \tag{2.5}$$

where V^{1-l} is the one-loop corrections to the scalar potential. While the condition

$$\widetilde{m}_0^2 + \lambda_0\upsilon^2/2 + \eta_{01}\upsilon_1^2/2 + \frac{1}{S_0}\frac{\partial}{\partial S_0} V^{1-l}\Big|_{\tilde{h}=\upsilon, \chi_1=\upsilon_1, S_0=0.} > 0, \tag{2.6}$$

JHEP02(2014)042

should be fulfilled in order that the potential does not develop a vev in the direction of S_0. In fact, the conditions (2.6) are not enough to guaranty the vacuum being (v, v_1); one must require that the Jacobian must be positive, which is equivalent to the fact that the two mass-squared eigenvalues are positive. In addition, we impose the vacuum stability condition

$$\lambda\eta_0\eta_1 - 9\eta_0\lambda_1^2 - 9\lambda\eta_{01}^2 - 9\eta_1\lambda_0^2 + 54\lambda_0\lambda_1\eta_{01} > 0, \tag{2.7}$$

where λ, η_1 and η_0 must be strictly positive, while λ_0, λ_1 and η_{01} could have negative values within the condition (2.7). Moreover, λ, η_1 η_0, λ_0, λ_1 and η_{01} must remain perturbative.

The spontaneous breaking of the electroweak and the $\mathbb{Z}_2$ symmetries introduces the two vacuum expectation values v and v_1 respectively. With the value of v being fixed experimentally to 246 GeV from W gauge boson mass, the model has ten parameters. The minimization conditions of the effective potential allows one to eliminate μ^2 and μ_1^2 in favor of (v, v_1). Then, we are left with eight parameters: λ, λ_0, λ_1, η_0, η_1, η_{01}, v_1 and m_0. However, the DM self-coupling constant η_0 does not enter the calculations of the lowest-order processes of this work, so effectively, we are left with seven input parameters.

The physical Higgs scalars h_1 and h_2, with masses m_1 and m_2 (with $m_1 < m_2$), are related to the excitations of the neutral component of the SM Higgs doublet field, $\mathrm{Re}(H^{(0)}) = (v + \widetilde{h})\sqrt{2}$, and the field $\chi_1 = \widetilde{\chi}_1 + v_1$ through a mixing angle θ. The scalars $\widetilde{h}$ and $\widetilde{\chi}_1$ are not the interacting fields but components of the eigenstates h_1 and h_2 which are obtained after the electroweak and the $\mathbb{Z}_2$ symmetries are spontaneously broken. Then the interactions of the DM candidate with the scalar sector that is relevant to the relic density, are not these in (2.4), but instead, their modification

$$\begin{pmatrix} h_1 \\ h_2 \end{pmatrix} = \begin{pmatrix} \cos\theta & \sin\theta \\ -\sin\theta & \cos\theta \end{pmatrix} \begin{pmatrix} \widetilde{h} \\ \widetilde{\chi}_1 \end{pmatrix}, \tag{2.8}$$

as shown in (2.9). In our work, the CP-even scalar masses and the mixing angle are estimated at one-loop. Here the quartic interactions get modified and new cubic interactions emerge [16–18]. The couplings of the h_1 and h_2 with fermions and gauge fields are just the projections of the doublets couplings using (2.8). The scalar potential that emerges after the electroweak symmetry breaking is given as a function of scalar eigenstates by

$$\begin{aligned} V(h_1, h_2, S_0) = {} & \frac{m_0^2}{2}S_0^2 + \frac{m_1^2}{2}h_1^2 + \frac{m_2^2}{2}h_2^2 \\ & + \frac{\lambda_{001}^{(3)}}{2}S_0^2 h_1 + \frac{\lambda_{002}^{(3)}}{2}S_0^2 h_2 + \frac{\lambda_{111}^{(3)}}{6}h_1^3 + \frac{\lambda_{222}^{(3)}}{6}h_2^3 + \frac{\lambda_{112}^{(3)}}{2}h_1^2 h_2 + \frac{\lambda_{122}^{(3)}}{2}h_1 h_2^2 \\ & + \frac{\eta_0}{24}S_0^4 + \frac{\lambda_{1111}^{(4)}}{24}h_1^4 + \frac{\lambda_{2222}^{(4)}}{24}h_2^4 + \frac{\lambda_{0011}^{(4)}}{4}S_0^2 h_1^2 + \frac{\lambda_{0022}^{(4)}}{4}S_0^2 h_2^2 + \frac{\lambda_{0012}^{(4)}}{2}S_0^2 h_1 h_2 \\ & + \frac{\lambda_{1112}^{(4)}}{6}h_1^3 h_2 + \frac{\lambda_{1122}^{(4)}}{4}h_1^2 h_2^2 + \frac{\lambda_{1222}^{(4)}}{6}h_1 h_2^3, \end{aligned} \tag{2.9}$$

where the triple and quartic coupling are given in appendix A. In our analysis we require that:

(i) all the dimensionless quartic couplings to be $\ll 4\pi$ for the theory to remain perturbative,

JHEP02(2014)042

(ii) they have to be chosen in such a way that the ground state stability is insured;

(iii) and we assume that the DM mass lies up to 1 TeV.

In our work, we consider the following values for the free parameters;

$$\begin{aligned} &\lambda, \eta_0, \eta_1, |\lambda_0|, |\lambda_1|, |\eta_{01}| < 3 \\ &20 < \frac{\upsilon_1}{\text{GeV}} < 2000, \quad 1 < \frac{m_0}{\text{GeV}} < 1000, \end{aligned} \tag{2.10}$$

and we make random choices taking into account the value of the relic density lying in the physical interval (3.3) and being not in conflict with direct detection DM experiments. Also, one of the CP even scalars mass lies around 123.5–127.5 GeV, with couplings to SM fermions and gauge bosons that are similar to the SM by more than $\epsilon \gtrsim 90\%$, where ϵ is $\cos^2\theta$ or $\sin^2\theta$ depending if h_1 or h_2 is the SM-like Higgs, respectively.

For our numerical illustration, we define the following two scenarios: A and B where the SM-like Higgs is h_1 and h_2 respectively. In addition, the invisible decay channel in case A $h_1 \to 2DM$ could be open up to 20%, while both $h_2 \to 2DM$ and $h_2 \to h_1 h_1$ should not exceed together 20% in case B. In fact, the former constraint on the invisible decay originates from global fit analysis to ATLAS and CMS data [20–26]. When deriving this limit in a global analysis, it is assumed that the Higgs boson has similar couplings to fermions and gauge bosons as in the SM and additional invisible decay modes. For instance, if the effective gluon-gluon-Higgs, γ-γ-Higgs or Higgs couplings to fermions are considered, the Higgs couplings to gauge bosons are modified, and therefore the above limit could be exceeded [25, 26]. Therefore, in our work, we consider the conservative choice $B(h \to invisible) \leq 20\%$. Recently, both ATLAS and CMS have searched for invisible decay of the Higgs. Assuming the Higgs-strahlung SM cross section for $pp \to ZH$ with 125 GeV SM Higgs boson, ATLAS exclude with 95% confidence level an invisible branching fraction of the Higgs larger than 65% and CMS obtain similar result [27]. CMS also looks for invisible decay of the Higgs through vector boson fusion process and exclude an invisible branching fraction of the Higgs larger than 69% [28]. When data from $pp \to ZH$ and VBF are combined the limit becomes 54% [28].

In our numerical scans, we will consider the parameter values that:

- ensure that one CP-even scalar is the SM-like by more than 90%,
- give the right amount of the DM relic density,
- do not conflict the direct detection DM experiments such as CDMSII [29, 30] and Xe100 [31, 32],
- in case A, the heavy scalar h_2 escapes the ATLAS [1] and CMS [2] bounds; and in case B, the light Higgs escapes the LEP constraints [33];
- and the invisible SM-like Higgs decay channel should not exceed 20%.

JHEP02(2014)042

3 Dark matter & detection

In the framework of the thermal dynamics of the Universe within the standard cosmological model [34, 35], the WIMP relic density is related to its annihilation rate by the familiar relation:

$$\Omega_D \bar{h}^2 = \frac{1.07 \times 10^9 x_f}{\sqrt{g_*} m_{\rm Pl} \langle \upsilon_{12} \sigma_{\rm ann} \rangle \, {\rm GeV}}, \tag{3.1}$$

with

$$x_f = \ln \frac{0.038 \; m_{\rm Pl} m_0 \langle \upsilon_{12} \sigma_{\rm ann} \rangle}{\sqrt{g_* x_f}}. \tag{3.2}$$

The notations are as follows: the quantity $\bar{h}$ is the Hubble constant in units of $100\, km \times s^{-1} \times Mpc^{-1}$, the quantity $m_{\rm Pl} = 1.22 \times 10^{19}\,{\rm GeV}$ the Planck mass, m_0 the DM mass, $x_f = m_0/T_f$ the ratio of the DM mass to the freeze-out temperature T_f and g_* the number of relativistic degrees of freedom with mass less than T_f. The quantity $\langle \upsilon_{12} \sigma_{\rm ann} \rangle$ is the thermally averaged annihilation cross section of a pair of two DM particles multiplied by their relative velocity in the center-of-mass reference frame [16–18]. When considering the current value for the DM relic density [36]

$$\Omega_D \bar{h}^2 = 0.1187 \pm 0.0017; \tag{3.3}$$

and taking the approximate values of $x_f \approx 19.2 \sim 21.6$ and $m_0 \approx 10 \sim 100$ GeV, we get

$$\langle \upsilon_{12} \sigma_{\rm ann} \rangle = (1.9 \pm 0.2) \times 10^{-9} \; {\rm GeV}^{-2}. \tag{3.4}$$

The value in (3.4) for the DM annihilation cross section translates into a relation between the parameters of a given theory entering the calculated expression of $\langle \upsilon_{12} \sigma_{\rm ann} \rangle$, hence imposing a constraint on these parameters will limit some of the possible range of DM masses. These constraints can be exploited to examine aspects of the theory like perturbativity, while at the same time reducing the number of parameters by one. However, since we will consider a wide range for the DM mass, $1 \sim 1000\,{\rm GeV}$, the ratio x_f will be estimated numerically using (3.1), especially for small mass values. Depending on how heavy/light is the DM candidate, its main annihilation channel will be to fermion pairs $f\bar{f}$ ($b\bar{b}$, $c\bar{c}$, $\tau\bar{\tau}$, or $\mu\bar{\mu}$), but for very large mass values, the channels $h_1 h_1$, $h_1 h_2$, $h_2 h_2$, WW, WW^*, ZZ, ZZ^* and $t\bar{t}$ could be also important. All the explicit formula of the annihilation cross section are given in [16–18].

During previous years, experiments such as CDMS II [29, 30], XENON 10/100 [31, 32] and CoGeNT [37] have been searching for signal of elastic scattering of a DM WIMP off nucleon targets in deep underground. Although, no unambiguous signal has been seen yet, they yielded increasingly stringent exclusion bounds on the DM-nucleon elastic scattering total cross section $\sigma_{\rm det}$ in terms of the DM mass m_0. The direct detection cross section for the scattering of S_0 (the DM candidate in this model) off nucleon, $\sigma_{\rm det}$, is given by [16–19]

$$\sigma_{\rm det} = \frac{g_{HNN}^2 m_N^2}{4\pi (m_N + m_0)^2} \left[\frac{\lambda_{001}^{(3)} \cos\theta}{m_1^2} - \frac{\lambda_{002}^{(3)} \sin\theta}{m_2^2} \right]^2, \tag{3.5}$$

JHEP02(2014)042

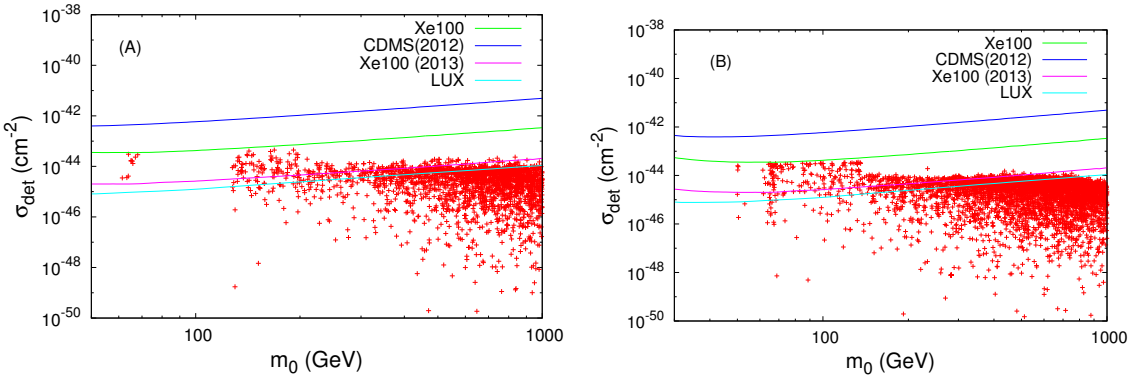

Figure 1. The direct detection cross section versus the DM mass compared to the recent Xe100 and LUX results, where the left and right panels correspond to the cases A and B respectively. It is clear that all the considered benchmarks are not in conflict with previous experimental bounds such as Xe100 (2012) and CDMSII (2012).

where m_N is the nucleon mass, $\lambda^{(3)}_{00i}$ is the coupling constants of $h_i S_0^2$ given in appendix A, and g_{HNN} is the effective Higgs-nucleon coupling**,** which is estimated based on heavy baryon chiral perturbation theory to be $g_{HNN} \simeq 1.5 \times 10^{-3}$ [38–40], whereas lattice calculations give somehow smaller values [41, 42].

In our work, the free parameters are chosen in such a way that the spectrum of the scalar sector has a SM Higgs like particle of 125 GeV, and the relic density of S_0 is consistent with the Planck data [36]. As it is shown in figure 1, we find that for most of the benchmarks, the elastic scattering cross section $\sigma_{\rm det}$ is below $10^{-45}\, cm^2$, i.e., below all the experimental bounds including the new one from Xe100 as well the latest LUX results [43], especially for DM masses larger than 125 GeV for case A; and 50 GeV for case B.

This behavior could be due to the cancelation between the two terms inside the bracket in eq. (3.5) or/and to the scaling of $\sigma_{\rm det}$ as the inverse square of m_0 which results in the suppression of the heavy DM event rate. However, for DM lighter than 30 GeV, the invisible Higgs decay fraction exceeds 20%, and so it is in conflict with ATLAS and CMS data.

4 The triple Higgs coupling

With the discovery of the Higgs-like particle at ATLAS and CMS with a mass in the range 125–126 GeV, and in order to establish the Higgs mechanism for the electroweak symmetry breaking we need to measure not only Higgs couplings to fermions and gauge bosons but also the triple and quartic self-coupling of the Higgs boson which are necessary for Higgs potential reconstruction. The measurement of the triple and quartic couplings, if precise enough, can help distinguishing between various SM extensions. The Triple Higgs self-coupling can be, in principle, measured directly in pair-production of Higgs boson at the LHC with high luminosity option [44, 45] and/or at e^+e^- International Linear Collider [14].

At the LHC, it is rather difficult to reconstruct the triple coupling of the Higgs because of the smallness of the cross section $gg \to hh$ as well as the large associated QCD

JHEP02(2014)042

background. Several parton level analysis have been devoted to this process with the following final states: $hh \to W^+W^-W^+W^-$ (which would lead to same sign leptons) [46, 47], $hh \to b\bar{b}W^+W^-$ [48], $hh \to b\bar{b}\gamma\gamma$ [49] and $hh \to b\bar{b}\tau^+\tau^-$ [48]. The last two processes seem to be very promising for High luminosity at the LHC. The authors in ref. [50] used the recent jet substructure techniques to study the Higgs pair production and the Higgs pair production in association with hard jet, where it is found that $b\bar{b}\tau^+\tau^-$ and $b\bar{b}\tau^+\tau^- + jet$ channels can be used to constrain the Triple Higgs self-coupling in the SM.

On the other hand, at the ILC, the process $e^+e^- \to Zhh \to l^+l^-b\bar{b}b\bar{b}$ has been investigated with 500 GeV center of mass energy with 1 ab^{-1} luminosity and it turns out that this process can be useful for measuring the Higgs self-coupling at the ILC [14].

In our study, the Triple Higgs self-couplings are estimated by taking the third derivatives of the effective potential at one-loop using the exact formulae given in appendix B, where we show how the renormalization scale disappears in favor of measured quantities. In our model, the deviation of the Triple Higgs self-coupling from the SM value can not come only from the modification of Higgs couplings to top quarks through the reduction factor ϵ (see eq. (B.11)), but also comes from new contributions of the other Higgs scalar and the DM candidate. In the rest of this section, for both cases A and B, we estimate the magnitude of different scalar triple couplings at one-loop and their deviation from the SM value. In what follows, the renormalization scale is taken to be the Higgs mass 125 GeV.

Case A: h_1 SM-like. In this case, h_1 is the SM-like while h_2 is dominated by singlet component. The relevant Triple Higgs self-couplings are $\lambda_{h_1h_1h_1}$, $\lambda_{h_1h_1h_2}$ and $\lambda_{h_1h_2h_2}$, where the first one corresponds to λ_{hhh} in the SM case. The other two couplings $\lambda_{h_1h_1h_2}$ and $\lambda_{h_1h_2h_2}$ have at least one h_1 leg which could give access to an associate production h_2h_1 or double production h_2h_2 through: $pp \to h_1^* \to h_1h_2$, $pp \to h_1^* \to h_2h_2$ at the LHC or $e^+e^- \to Zh_1^* \to Zh_1h_2$, $e^+e^- \to Zh_1^* \to Zh_2h_2$ at the ILC.

In order to illustrate the magnitude of the one-loop corrected triple Higgs couplings, we show in figure 2-left the triple SM-like Higgs coupling versus its tree-level value. It is clear that only the coupling $\lambda_{h_1h_1h_1}$ which receives significant corrections at the one-loop level and make it larger than its corresponding tree level value. Also one has to mention that its value is the smallest one with respect to the other ones: $\lambda_{h_1h_2h_2}$ and $\lambda_{h_1h_1h_2}$. Note that the value of $\lambda_{h_2h_2h_2}$ (which is not shown here) could be much larger than the others, i.e. up to $\lambda_{h_2h_2h_2} \sim 8 \times v$.

In order to show the effect of these new contributions on this triple coupling $\lambda_{h_1h_1h_1}$, we define the following quantity $\Delta_{h_1h_1h_1} = (\lambda_{h_1h_1h_1} - \lambda_{hhh}^{\rm SM})/\lambda_{hhh}^{\rm SM}$, which represents the relative enhancement on the triple Higgs coupling at one-loop with respect to the same quantity estimated at one-loop in the SM for the recently measured Higgs mass.

In figure 2-right, we show $\Delta_{h_1h_1h_1}$ as a function of the heavy scalar mass m_2. It is clear that in this case, the one-loop corrections to the SM-like Higgs h_1 could have an enhancement greater than 40%. Since we have subtracted the SM contribution at one-loop, this enhancement is then attributed to the new contributions of h_2 and S_0.

Case B: h_2 SM-like. In the case where h_2 is SM-like, h_1 is dominated by singlet component and according to our convention is lighter than h_2. In this case, the rele-

JHEP02(2014)042

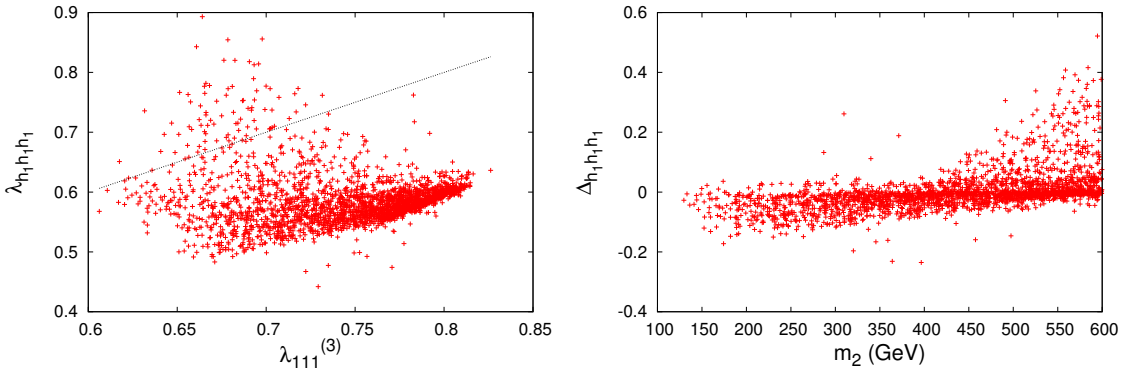

Figure 2. Left panel: the SM-like triple Higgs coupling versus its tree-level value in units of the EW vev value for randomly chosen sets of parameters, where the SM-like Higgs is defined according to case A. Right panel: the relative enhancement on the SM-like triple Higgs coupling of with respect to the SM value versus the mass of the heavy scalar m_2 for the same sets of parameters.

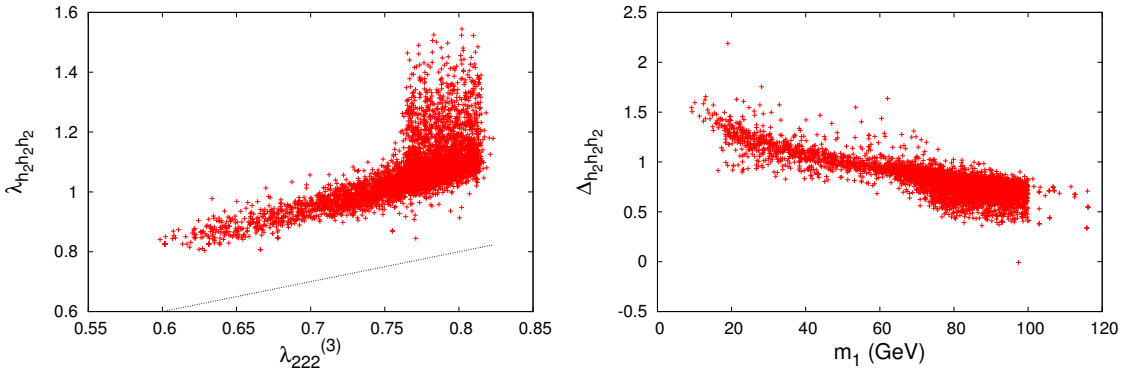

Figure 3. Left panel: the triple Higgs couplings in absolute values, in units of the EW vev value, versus its tree-level value for randomly chosen sets of parameters, where the SM-like Higgs is defined according to case B. Right panel: the relative enhancement on the SM-like Triple Higgs coupling of h_2 with respect to the SM case versus the mass of the light scalar m_1 for randomly chosen sets of parameters.

vant triple Higgs coupling is $\lambda_{h_2h_2h_2}$, which corresponds to λ_{hhh} in the SM case. Like in case A, the other two couplings $\lambda_{h_1h_2h_2}$ and $\lambda_{h_1h_1h_2}$ have at least one h_2 leg which could give access to an associate production h_2h_1 or double production h_1h_1 through the processes: $pp \to h_2^* \to h_1h_2$, $pp \to h_2^* \to h_1h_1$ at the LHC or $e^+e^- \to Zh_2^* \to Zh_1h_2$, $e^+e^- \to Zh_2^* \to Zh_1h_1$ at an e^+e^- machine. Figure 3-left shows the one-loop correction effects to the SM-like triple coupling versus its tree-level value.

In this case, the one-loop corrections to the coupling $\lambda_{h_2h_2h_2}$ make it larger than its corresponding tree level value. In figure 3-right, we plot the quantity $\Delta_{h_2h_2h_2} = (\lambda_{h_2h_2h_2} - \lambda_{hhh}^{\rm SM})/\lambda_{hhh}^{\rm SM}$ as a function of the light scalar mass m_1.

We see that in this case, the one-loop corrections to the SM-like Higgs h_2 could enjoy large enhancement which lies between few 40% and 100% for $10\,\text{GeV} < m_1 < 100$ GeV.

JHEP02(2014)042

This effect is even amplified and can reach 150% and more when we cross the threshold $h_2 \to h_1 h_1$ region. This kind of large radiative corrections have been also reported in the framework of two Higgs doublet model [51].

5 Higgs phenomenology

In this section, we will discuss h_1 and h_2 phenomenology.

5.1 Higgs decays

The partial decay widths of the two Higgs scalars $h_{1,2}$ into SM particles such as $f\bar{f}$, WW (WW^*) and ZZ (ZZ^*) is just the SM rate multiplied by $\epsilon = \cos^2\theta, \sin^2\theta$, depending on whether h_1 or h_2 is the decaying particle. This ϵ factor apply also for loop mediated process such as $h_i \to \gamma\gamma, Z\gamma, gg$. The decay rate of $h_2 \to h_1 h_1$ is given by

$$\Gamma\left(h_2 \to h_1 h_1\right) = \frac{\left(\lambda_{112}^{(3)}\right)^2}{32\pi m_2}\left(1 - \frac{4m_1^2}{m_2^2}\right)^{\frac{1}{2}} \Theta\left(m_2 - 2m_1\right), \tag{5.1}$$

and the light/heavy Higgs decay to DM final state S_0 is

$$\Gamma\left(h_i \to S_0 S_0\right) = \frac{\left(\lambda_{00i}^{(3)}\right)^2}{32\pi m_i}\left(1 - \frac{4m_0^2}{m_i^2}\right)^{\frac{1}{2}} \Theta\left(m_i - 2m_0\right). \tag{5.2}$$

Moreover, in this model h_2 can also decay to Triple Higgs h_1 if kinematically allowed: $h_2 \to h_1 h_1 h_1$ which would require $m_2 > 3m_1$. This decay channel has three contributions: quartic term $h_2 h_1 h_1 h_1$, contribution mediated by off-shell h_1^*: $h_2 \to h_1 h_1^* \to h_1 h_1 h_1$ and a contribution mediated by off-shell h_2^*: $h_2 \to h_1 h_2^* \to h_1 h_1 h_1$. This decay, even if it is open could not compete with the 2 body phase space decay $h_2 \to h_1 h_1$ due to the 3 body phase space suppression.

The reduction factor for the SM final state process $h_1 \to X_{\rm SM}$ is given by

$$\begin{aligned} R_{X_{\rm SM}}\left(h_1\right) &= G\frac{B(h_1 \to X_{\rm SM})}{B^{\rm SM}(h \to X_{\rm SM})} \\ &= \frac{c^4 \Gamma_{\rm tot}^{\rm SM}\left(h_1\right)}{c^2 \Gamma_{\rm tot}^{\rm SM}\left(h_1\right) + \Gamma(h_1 \to S_0 S_0)}, \end{aligned} \tag{5.3}$$

with the G-factor is given by

$$G = \frac{\sigma(gg \to h_1)}{\sigma^{\rm SM}(gg \to h)} = c^2. \tag{5.4}$$

The reduction factor for $h_2 \to X_{\rm SM}$ is

$$R_{X_{\rm SM}}\left(h_2\right) = \frac{s^4 \Gamma_{\rm tot}^{\rm SM}\left(h_2\right)}{s^2 \Gamma_{\rm tot}^{\rm SM}\left(h_2\right) + \Gamma(h_2 \to X_{NSM})}, \tag{5.5}$$

where X_{NSM} denotes all the non SM final states such as $h_1 h_1$, $h_1 h_1 h_1$, $S_0 S_0$ or $h_1 S_0 S_0$. For case B, due to the fact that $R_{X_{\rm SM}}\left(h_2\right)$ is proportional to s^2, all values of $s^2 < 0.1$ will be in perfect agreement with ATLAS and CMS data.

JHEP02(2014)042

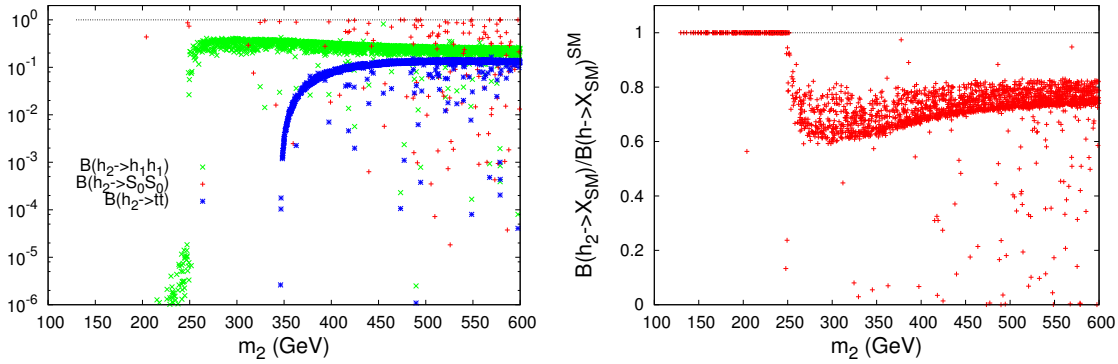

Figure 4. Left panel: the branching ratios of the decay channels $h_2 \to t\bar{t}$, $h_2 \to h_1 h_1$ and $h_2 \to S_0 S_0$ versus its mass. Right panel: the branching ratio of the heavy Higgs to the SM particles final states versus the heavy Higgs mass; scaled by the same quantities evaluated in the SM.

In the following plots, we will show our numerical results illustrating different physical quantities for the case A previously introduced where h_1 is the SM-like Higgs.

In figure 4, we show the branching ratios of h_2-decay to SM (right) and non-SM (left) final states. In figure 4(left), we illustrate the branching ratio of the heavy Higgs h_2 into $t\bar{t}$, $S_0 S_0$ and $h_1 h_1$ as a function of m_2. It is clear that for $m_2 \approx 125 - 150\,\text{GeV}$, h_2 will decay dominantly to SM particles such as $b\bar{b}$, WW^* and ZZ^*, if the decay $h_2 \to S_0 S_0$ is kinematically forbidden. Once $h_2 \to S_0 S_0$ is open, it dominates all the other decays. For the range $m_2 \approx 150{-}250\,\text{GeV}$, we can see the opening of the three body phase space channel $h_2 \to h_1 h_1^* \to h_1 f \bar{f}$ which is rather small (less than 10^{-4}). However, once $m_2 \geq 250\,\text{GeV}$ the on-shell decay $h_2 \to h_1 h_1$ is open and compete with $h_2 \to S_0 S_0$. As one can see, the channels $h_2 \to h_1 h_1$ and $h_2 \to t\bar{t}$ can reach 40% and 10% branching ratio respectively.

As a summary, if the invisible channel $h_2 \to S_0 S_0$ does not dominate, one can say that:

(1) for $m_{\mathbf{2}} < 250\,\text{GeV}$, $h_{\mathbf{2}}$ Higgs decays similar to the SM case,

(2) for $250\,\text{GeV} < m_{\mathbf{2}} < 400\,\text{GeV}$, it decays similar to the SM by 60% and to $h_{\mathbf{1}} h_{\mathbf{1}}$ by 40 %;

(3) for $m_{\mathbf{2}} > 400\,\text{GeV}$, $B(h_2 \to h_1 h_1)$ becomes 30% and $B(h_2 \to t\bar{t})$ becomes important as 10%.

At the end, we give the total decay width for the two CP-even scalars in both cases in figure 5. It is well known that the SM Higgs with a mass of 125 GeV has a very narrow width which is $\Gamma_h \approx 4\,\text{MeV}$.

In case A where h_1 is the SM-like, the total width of h_1 is in the range 3.7–4.6 MeV while the total width of h_2 can be located between 10^{-3} and 10^4 MeV. A very narrow width of h_2 means that Higgs to Higgs decays of h_2 such that $h_2 \to h_1 h_1$ and $h_2 \to S_0 S_0$ are closed and only h_2 decays to SM particles are open which are suppressed because h_2 is dominated by singlet.

JHEP02(2014)042

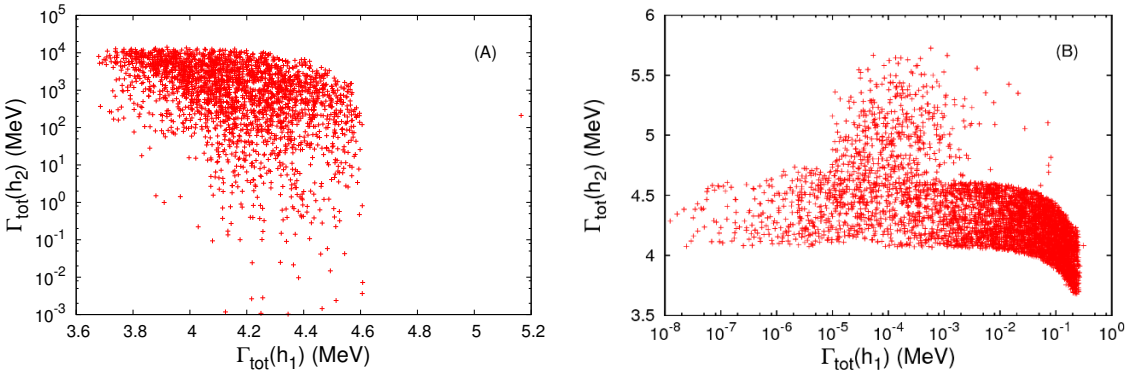

Figure 5. The total decay width of the SM-like Higgs versus the non SM-like Higgs in both cases A (left) and B (right).

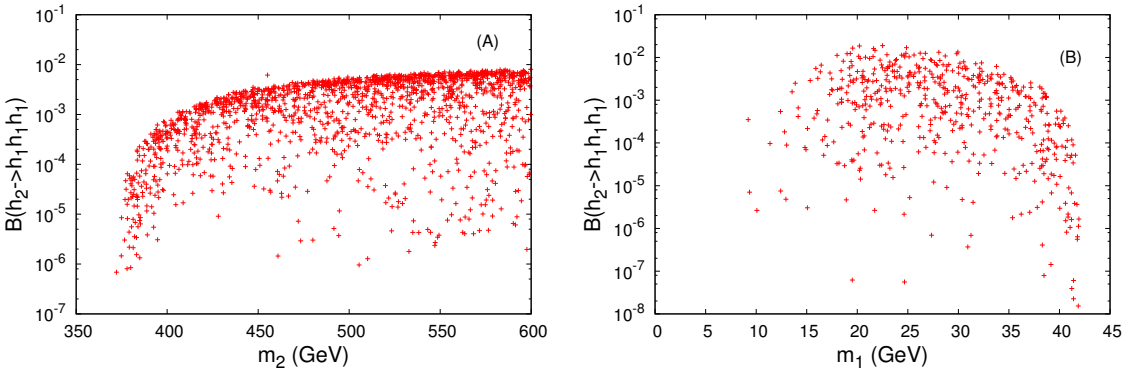

Figure 6. The branching ratio B($h_2 \to h_1h_1h_1$) versus the non SM-like Higgs mass for both cases A (up-left) and B (up-right).

In case B where h_2 is the SM-like, its total width is very narrow (3.5–4.6 MeV) if $h_2 \to S_0S_0$ and $h_2 \to h_1h_1$ are closed. Once these two channels are open, the total width of h_2 grows up to 5.7 MeV. The total width of h_1 which is dominated by singlet is rather small, less than 0.2 MeV.

For some benchmarks in both cases, the decay $h_2 \to h_1h_1h_1$ is kinematically possible, and it is important to estimate how large is this branching ratio. In figure 6, we show $B(h_2 \to h_1h_1h_1)$ versus m_2 (m_1) for case A (B).

It is clear that this branching ratio is in the order of $\mathcal{O}(10^{-2})$ and below. We stress here that in case where h_2 is the SM-like Higgs boson, which has quite substantial cross section, it may be possible to measure such 3-body phase space decay with a branching ratio of the order 10^{-2}.

For case B, we show in figure 7 the branching ratio for $h_2 \to h_1h_1$ (including $h_2 \to h_1h_1^*$) versus the light Higgs mass; and the resonant production cross section of both $gg \to h_2 \to h_1h_1$ and $gg \to h_2 \to h_1h_1h_1$ versus the light Higgs mass is shown in figure 8.

JHEP02(2014)042

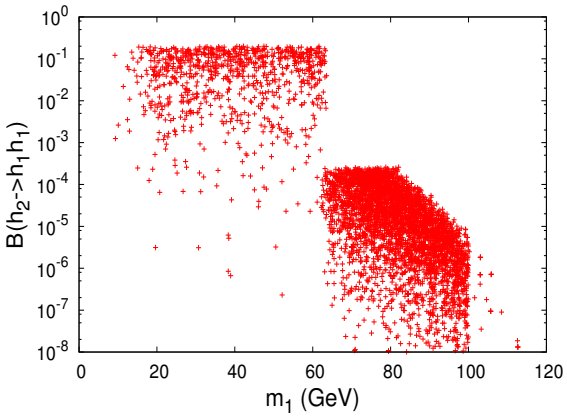

Figure 7. The branching ratio B($h_2 \to h_1 h_1$) versus the non SM-like Higgs mass for case B.

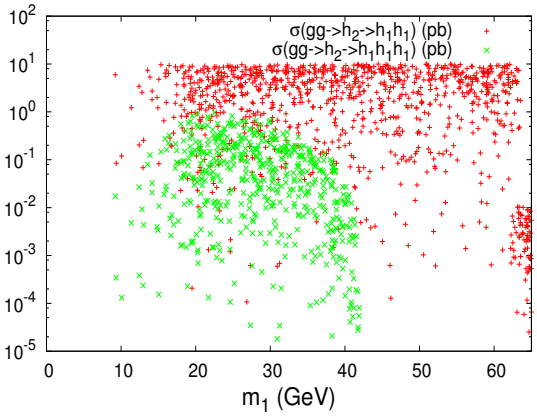

Figure 8. The resonant production cross section for double and triple singlet h_1 as a function of m_1 for case B. The red points are for $\sigma(gg \to h_2) \times B(h_2 \to h_1 h_1)$, and the green ones are for $\sigma(gg \to h_2) \times B(h_2 \to h_1 h_1 h_1)$, all cross sections are in pb.

5.2 Higgs production

Same as in the SM, at the LHC the dominant production cross section for the SM like Higgs h_1 or h_2 would be dominated by gluon fusion process which is mediated by the top loops. The cross section rate for a single Higgs production will be simply modified by the mixing angle c^2 or s^2 depending on h_1 or h_2 production:

$$\begin{aligned} \sigma(gg \to h_1) &= c^2 \times \sigma(gg \to h_{\rm SM}), & \sigma(gg \to h_2) &= s^2 \times \sigma(gg \to h_{\rm SM}) \\ \sigma(pp \to V h_1) &= c^2 \times \sigma(pp \to V h_{\rm SM}), & \sigma(pp \to V h_2) &= s^2 \times \sigma(pp \to V h_{\rm SM}) \end{aligned} \tag{5.6}$$

It is clear that in case A where h_1 is the SM-like and dominated by doublet component $c \approx 1$ and h_2 is dominated by singlet component. In this case, the cross section $\sigma(gg \to h_1)$ (or $\sigma(pp \to V h_1)$) will be typically close to SM one while $\sigma(gg \to h_2)$ (or $\sigma(pp \to V h_2)$) will be suppressed by s^2 which is rather small in this case. Same thing apply for the case B.

JHEP02(2014)042

$(\sin\theta,\ m_1,\ m_2,\ m_0)$	λ_{111}	λ_{112}	λ_{122}	$B(h_2 \to h_1 h_1)$	$\sigma^{\rm LHC}(h_1 h_1)$	$\sigma^{\rm LHC}(h_1 h_2)$	$\sigma^{\rm ILC}(Z h_1 h_1)$
(0.041, 125.9, 252.2, 415.2)	195.1	−15.6	18.2	0.1039	24.3	0.045	0.157
	143.8	−17.7	17.0	0.0819	30.3	0.041	0.134
(−0.16, 124.4, 249.2, 658.9)	183.2	66.2	−49.3	0.0349	28.9	0.77	0.185
	134.1	76.3	−44.9	0.0265	35.6	0.65	0.175
(0.243, 124.1, 247.8, 639.7)	174.4	−79.8	75.3	7.00×10^{-4}	22.37	1.40	0.167
	129.2	−92.7	75.1	5.18×10^{-4}	26.6	1.22	0.155
(−.23, 125.6, 550.4, 668.4)	178.6	311.5	−86.5	0.3057	105.5	0.16	0.11
	160	351	−45	0.2573	115	0.17	0.103
(0.262, 124.3, 450.6, 802.3)	171.9	−205.4	319.2	0.1942	224.8	0.47	0.102
	140	−198	311	0.2065	222.6	0.46	0.09
(−.26, 124.1, 295.5, 920.3)	169	140	−105	0.4890	387	1.5	2.4
	131	165	−80	0.4074	407	1.18	2.05
(−.31, 125.5, 406.1, 662)	165	258	−103	0.3855	478	0.85	0.19
	149	297	−65	0.3215	511	0.78	0.17

Table 1. Benchmarks scenario for case A, all masses, couplings λ_{ijk} are in GeV. The LHC energy at 14 TeV and the ILC at 500 GeV, all cross sections are in fb. In the SM, $\sigma^{LHC}(pp \to hh) = 25.4$ fb at 14 TeV and $\sigma^{ILC}(e^+e^- \to Zhh) = 0.14$ fb at 500 GeV for $m_h = 125$ GeV. The first value for triple couplings, branching ratio $B(h_2 \to h_1 h_1)$ and cross sections corresponds to the Leading Order (LO) while the second one corresponds to improved LO by taking the triple coupling at one-loop level.

For the double Higgs production which is a good probe for Triple Higgs self-coupling, we will evaluate $gg \to h_i h_j$ for the LHC and $e^+e^- \to Z h_i h_j$ for the ILC in some benchmark scenarios which are given in table 1 and table 2. We remind here that in the SM, the double Higgs production at the LHC $gg \to hh$ proceeds at one-loop level trough vertex and boxes contributions (top exchange) which interfere destructively in the total cross section. In the two singlets model under consideration, the vertex contributions can be mediated by the 2 Higgs scalars $h_{1,2}$: $gg \to h^*_{1,2} \to h_i h_j$ which could give some resonant effects from $h_2 \to h_1 h_1$.

5.2.1 Resonant production of the SM-like Higgs

In case A, where h_1 is the SM-like Higgs and h_2 is dominated by singlet component. In this case the processes $gg \to h^*_1, h^*_2 \to h_1 h_1$ or $e^+e^- \to Z h^*_1, Z h^*_2 \to Z h_1 h_1$ could enjoy the resonance production of $h_1 h_1$ through the decay $h_2 \to h_1 h_1$ which could have a branching ratio up to 20% if open (see table 1). Similar behavior had been noticed for general two Higgs doublet model [52–54], portal model [55] and next minimal supersymmetric standard model [56, 57].

As one can see from table 1, the production cross section of $h_1 h_1$ could be substantial due to resonant contribution from $h_2 \to h_1 h_1$. In the narrow width approximation of h_2, the pair production of h_1 could be approximated by $\sigma(pp \to h_2) \times B(h_2 \to h_1 h_1)$. This product could be sizable if the singlet component s of h_2 is not very small and $B(h_2 \to h_1 h_1)$ not very suppressed.

In table 1, the benchmarks in lines 4, 5 and 7 correspond to the case where the decay $h_2 \to h_1 h_1 h_1$ is kinematically possible; however its branching ratio is 1.022×10^{-3}, 2.178×10^{-5} and 1.352×10^{-4}, for these benchmarks respectively. For case A, the branching ratio

JHEP02(2014)042

$(\sin\theta,\ m_1,\ m_2,\ m_0)$	λ_{112}	λ_{122}	λ_{222}	$B(h_2 \to h_1 h_1)$	$\sigma^{\rm LHC}(h_1 h_1)$	$\sigma^{\rm LHC}(h_2 h_2)$	$\sigma^{\rm ILC}(Z h_1 h_1)$
(0.98, 63, 126.2, 281.5)	16	34	−183.5	0.1171	3555	22.8	35.19
	13	17.5	−262.3	0.1696	2421	16.2	30.8
(0.999, 54.8, 124, 584.7)	4.8	3.46	−189.38	0.1842	3715.86	25.069	39.67
	4.9	1.2	−277	0.1718	3992	17	28
(−0.976, 85.5, 126.9, 263.4)	68.4	16	189.7	5.29×10^{-3}	0.92	21.95	0.0061
	73.2	3.47	252.3	4.61×10^{-3}	1.34	15.8	0.008
(−0.966, 87.2, 125.9, 480.3)	79.8	15.1	184.2	4.92×10^{-3}	0.868	21.33	0.008
	86.7	67.2	244.9	4.16×10^{-3}	1.39	16.4	0.01
(0.967, 94.5, 126.1, 191.4)	56.9	60.9	−171.2	5.06×10^{-4}	0.57	21.66	0.0005
	56.5	43	−226.2	5.13×10^{-4}	0.63	17.2	0.0005
(0.977, 82, 124.5, 862)	52.5	48.016	−174.509	4.36×10^{-3}	1.308	22.95	0.0017
	52.6	33.2	−231.8	4.35×10^{-3}	1.43	18	0.002

Table 2. Benchmarks scenario for case B, all masses, couplings λ_{ijk} are in GeV. The LHC energy at 14 TeV and the ILC at 500 GeV, all cross sections are in fb. The first value for triple couplings, branching ratio $B(h_2 \to h_1 h_1)$ and cross sections corresponds to the leading order (LO) while the second one corresponds to improved LO by taking the triple coupling at one-loop level.

$B(h_2 \to h_1 h_1)$, the coupling $\lambda_{h_1 h_1 h_2}$ and the cross sections $\sigma(pp \to h_1 h_1)$ and $\sigma(e^- e^+ \to Z h_1 h_1)$ could receive corrections up to 20%, 16%, 26% and 14%, respectively.

In case B, since h_2 is SM-like, the production $pp \to h_2 h_2$, will be roughly similar to SM, because in this case h_1 is lighter than h_2 and then $pp \to h_2 h_2$ can not benefit from the resonant production of h_1 to a pair of h_2. This can be seen in table 2. We stress here that by taking the values of the couplings λ_{122} and λ_{222} at one-loop level reduces slightly the cross sections as can be seen from table 2. In the first benchmark of table 2, improving the coupling λ_{112} by the one loop corrections can modify the Branching ratio $B(h_2 \to h_1 h_1)$ and the cross section $gg \to h_1 h1$ up to 45% and 32% respectively.

5.2.2 Singlet scalars production

As we have seen previously for case B, the decay $h_2 \to h_1 h_1$ could be open and its branching ratio could reach 20%. Using the fact that a SM-Higgs h_2 with 125 GeV will be copiously produced at 14 TeV LHC: $\sigma(pp \to h_2) \approx 50$ pb, one can have access to the following production for two singlet scalars:

$$\begin{aligned}\sigma(pp \to h_1 h_1) &\approx \sigma(pp \to h_2) \times B(h_2 \to h_1 h_1) \\ &\approx s^2 \times \sigma(pp \to h_{\rm SM}) \times B(h_2 \to h_1 h_1) \\ &\approx 9 \left[\frac{s^2}{0.9}\right] \left[\frac{B(h_2 \to h_1 h_1)}{0.2}\right] \text{(pb) for } m_2 = 125 \text{ GeV}, \end{aligned} \tag{5.7}$$

which is rather substantial if $B(h_2 \to h_1 h_1)$ is not suppressed. As it is illustrated in figure 8 (red points), the production cross section for double singlet h_1 could be substantial for large area of parameter space and can reach 10 pb which would lead to a visible signal if this scenario is realized.

JHEP02(2014)042

Same estimate for triple Higgs production at the LHC gives:

$$\begin{aligned}\sigma(pp \to h_1h_1h_1) &\approx \sigma(pp \to h_2) \times B(h_2 \to h_1h_1h_1)\\ &\approx s^2 \times \sigma(pp \to h_{\rm SM}) \times B(h_2 \to h_1h_1h_1)\\ &\approx 0.1 \left[\frac{s^2}{0.9}\right] \left[\frac{B(h_2 \to h_1h_1h_1)}{10^{-2}}\right] \text{(pb) for } m_2 = 125 \text{ GeV}, \end{aligned} \tag{5.8}$$

which is rather large compared to the Drell-Yann cross section for $2 \to 2$ processes. In figure 8 (green points), we illustrate the production cross section for triple singlet h_1 coming mainly from $\sigma(gg \to h_2) \times B(h_2 \to h_1h_1h_1)$. As it can be seen it turns out that this production channel could give a cross section up to 1 pb if the singlet h_1 is in the range 20–30 GeV. At the 14 TeV LHC run with 100 fb^{-1} luminosity, 1 pb cross section can leads to 10^5 raw events of $6b$ or $4b2\tau$ or $2b4\tau$ or 6τ without cuts.

Similarly, at the ILC we can have access to a pair of singlet scalars by producing first the SM Higgs h_2 which can decay with sizable branching ratio to a pair of singlet scalars. In the narrow width approximation of h_2, we have:

$$\begin{aligned}\sigma(e^+e^- \to Zh_1h_1) &\approx \sigma(e^+e^- \to Zh_2) \times B(h_2 \to h_1h_1)\\ &\approx s^2 \times \sigma(e^+e^- \to Zh_{\rm SM}) \times B(h_2 \to h_1h_1)\\ &\approx 21.5 \left[\frac{s^2}{0.9}\right] \left[\frac{B(h_2 \to h_1h_1)}{0.2}\right] (fb) \quad \text{for} \quad \sqrt{s} = 250 \text{ GeV}\\ &\approx 5.1 \left[\frac{s^2}{0.9}\right] \left[\frac{B(h_2 \to h_1h_1)}{0.2}\right] (fb) \quad \text{for} \quad \sqrt{s} = 500 \text{ GeV}. \end{aligned} \tag{5.9}$$

It is obvious, that at the ILC the cross section is more important near threshold production of Zh_2 which is close to 250 GeV. Since the process $e^+e^- \to Zh_2$ is mediated by s-channel Z exchange, the cross section is slightly suppressed for higher center of mass energy ≥ 500 GeV.

To have an idea about the order of magnitude of these cross sections both at the LHC-14 TeV and the ILC we give some numerical results in table 1 for case A and table 2 for case B. It is clear that both at LHC and ILC the double Higgs production can be larger or smaller than the corresponding SM one. In the cross sections for hadron collider, we include a K-factor $K = 2$ [58]. In case A, one can see that the cross section of a pair production of SM-like Higgs could exceed in some cases 100 fb, which would give more than 10^4 raw events for an integrated LHC luminosity of 100 fb^{-1} giving rise to $b\bar{b}b\bar{b}$ and $b\bar{b}\tau^+\tau^-$ final states with large transverse momentum. Observation of such large Higgs pair production cross sections would be a clear evidence for physics beyond the SM.

In case B, where h_1 is a singlet with a mass less than 125 GeV, it is clear from table 2 that pair production of singlet scalars could be substantial and the LHC cross sections could exceed 3 pb, giving more events than in the previous case. In case B, where h_2 is the SM-like, the lighter Higgs scalar h_1 decays to SM final states with the same branching ratios as the SM Higgs. Then, for benchmarks where the cross section $\sigma(pp \to h_1h_1)$ is around 10 pb, we will have the $b\bar{b}b\bar{b}$ final state. However, this final state suffers from a huge QCD background. The $b\bar{b}\tau^-\tau^+$, $b\bar{b}\gamma\gamma$ final states are promising one in the case of

JHEP02(2014)042

SM Higgs pair production [48, 49]. Since in our case, the production cross section is much higher than the production of a Higgs pair in the SM, a possible signal extraction could be performed with a very good efficiency. A more interesting final state is $\tau^-\tau^+\tau^-\tau^+$, which would give same sign dileptons if the τ's of the same electric charge decay leptonically. All these possible final states need a full Monte Carlo analysis which is out of the scope of the present study.

6 Conclusion

We have shown that the two-singlets model can accommodate a Higgs boson with a mass in the range 125–126 GeV together with the relic density and indirect detection constraints as well as all the recent measurements from ATLAS and CMS experiments. The model has three CP-even Higgs $h_{1,2}$, two of which are a mixture of doublet and a singlet components, while the third one is a singlet particle S_0 which plays the role of DM candidate. We studied both the cases where h_1 or h_2 is the SM-like Higgs; and investigated the effect of the extra Higgs bosons on the triple Higgs self-couplings. We have found that in the case where h_1 is the SM-like Higgs, the Triple Higgs self-coupling $h_1h_1h_1$ can receive a significant enhancement which could be greater than 40% for $m_2 > 600$ GeV. In the case where h_2 is the SM-like Higgs, the Higgs triple self-coupling $h_2h_2h_2$ receives an enhancement between 50% and 150%.

We have discussed that some of the Higgs pair h_ih_j could be produced either at the 14 TeV LHC with high luminosity option or at the future linear collider where the mass and the triple coupling of the Higgs could be measured with very good precision. We have also seen that when h_2 is the SM-like Higgs and h_1 is singlet dominated Higgs and lighter than h_2, one can produce either a pair of h_1 or triple h_1 through $\sigma(pp \to h_2) \times B(h_2 \to h_1h_1)$ or $\sigma(pp \to h_2) \times B(h_2 \to h_1h_1h_1)$ with substantial cross section. This will constitute an important mechanism for producing singlet scalars in this model. In the other case where h_1 is the SM-like Higgs and h_2 is the singlet scalar, we have seen that we can have a cross section of a Higgs pair h_1 which is more than one order of magnitude larger than the corresponding SM one. Observation of such large Higgs pair production would be a clear indication of physics beyond the SM.

Acknowledgments

The work of A. Ahriche is supported by the Algerian Ministry of Higher Education and Scientific Research under the PNR '*Particle Physics/Cosmology: the interface*', and the CNEPRU Project No. *D01720130042*. A. Arhrib would like to thank NSC-Taiwan for financial support during his stay at Academia Scinica where part of this work has been done.

A Cubic and quartic scalar couplings

The cubic and quartic terms are obtained after the symmetry breaking as couplings between the scalar eigenstates. Here we used a notation where the subscripts 0, 1 and 2 denote S_0,

JHEP02(2014)042

h_1 and h_2 respectively. The cubic couplings with dimension of a mass are

$$\begin{aligned}
&\lambda^{(3)}_{001} = c\lambda_0 v + s\eta_{01} v_1, \quad \lambda^{(3)}_{002} = c\eta_{01} v_1 - s\lambda_0 v,\\
&\lambda^{(3)}_{111} = c^3\lambda v + \frac{3}{2}s^2\lambda_1(cv_1 + sv) + s^3\eta_1 v_1,\\
&\lambda^{(3)}_{222} = c^3\eta_1 v_1 - 3cs\lambda_1(cv - sv_1) - s^3\lambda v,\\
&\lambda^{(3)}_{112} = c^3\lambda_1 v_1 + cs[c(2\lambda_1 - \lambda)v - s(2\lambda_1 - \eta_1)v_1] - s^3\lambda_1 v,\\
&\lambda^{(3)}_{122} = c^3\lambda_1 v - cs[c(2\lambda_1 - \eta_1)v_1 + s(2\lambda_1 - \lambda)v] + s^3\lambda_1 v_1,
\end{aligned} \tag{A.1}$$

and the quartic terms are

$$\begin{aligned}
&\lambda^{(4)}_{1111} = \lambda c^4 + 6\lambda_1 c^2 s^2 + \eta_1 s^4, && \lambda^{(4)}_{2222} = \eta_1 c^4 + 6\lambda_1 c^2 s^2 + \lambda s^4,\\
&\lambda^{(4)}_{0011} = \lambda_0 c^2 + \eta_{01} s^2, \quad \lambda^{(4)}_{0022} = \eta_{01} c^2 + \lambda_0 s^2, && \lambda^{(4)}_{012} = cs(\eta_{01} - \lambda_0),\\
&\lambda^{(4)}_{1112} = cs[(3\lambda_1 - \lambda)c^2 - (3\lambda_1 - \eta_1)s^2], && \lambda^{(4)}_{1122} = \lambda_1\left(c^2 - s^2\right)^2 - c^2 s^2(2\lambda_1 - \eta_1 - \lambda),\\
&\lambda^{(4)}_{1222} = cs[(\eta_1 - 3\lambda_1)c^2 - (\lambda - 3\lambda_1)s^2].
\end{aligned} \tag{A.2}$$

B The effective triple Higgs couplings

The effective triple Higgs couplings can be estimated as the third derivatives of the effective potential with respect the scalar CP-even eigenstates. For a general form of the effective potential

$$V\left(\tilde{h}\right) = -\sum_k \frac{\mu_k^2}{2}\tilde{h}_k^2 + \frac{\lambda_k}{24}\tilde{h}_k^4 + \sum_{i,k}\frac{\omega_{ik}}{4}\tilde{h}_i^2\tilde{h}_k^2 + V^{1-l}(\tilde{h}), \tag{B.1}$$

$$V^{1-l}\left(\tilde{h}\right) = \sum_{\alpha=\text{all fields}} \frac{n_\alpha m_\alpha^4(\tilde{h})}{64\pi^2}\left(\log\frac{m_\alpha^2(\tilde{h})}{\Lambda^2} - c_\alpha\right), \tag{B.2}$$

with $\omega_{ik} = 0$ for $k \leq i$, the effective triple Higgs couplings are given by

$$\lambda^{(3)}_{ijk} = \lambda^{(3-\text{tree})}_{ijk} + \frac{\partial^3}{\partial h_i \partial h_j \partial h_k}\left[\sum_\alpha \frac{n_\alpha m_\alpha^4(\tilde{h})}{64\pi^2}\left(\log\frac{m_\alpha^2(\tilde{h})}{\Lambda^2} - c_\alpha\right)\right], \tag{B.3}$$

where $\lambda^{(3-tree)}_{ijk}$ are the tree-level triple couplings in (A.1), c_α depends on the renormalization scheme; and $\tilde{h}$ are the CP-even scalars (like $\tilde{h}$ and χ_1 in our model) and h are the eigenstates after the symmetry breaking where

$$h_i = u_{ik}\tilde{h}_k, \ \tilde{h}_i = u^T_{ik}h_k = u_{ki}h_k, \tag{B.4}$$

and u_{ik} are the mixing matrix elements. In order to evaluate the second term in (B.3), we parameterize the field dependent masses as

$$m_\alpha^2(\tilde{h}) = m_\alpha^2\left[1 + \epsilon_\alpha\right], \tag{B.5}$$

JHEP02(2014)042

with ϵ in terms of the eigenstates h_i or the fields $\tilde{h}_i$; and can be expanded as

$$\begin{aligned}\epsilon_\alpha &\simeq \eta_{\alpha,i}h_i + \varsigma_{\alpha,ik}h_ih_k + \xi_{\alpha,ikl}h_ih_kh_l,\\ &\simeq \tilde{\eta}_{\alpha,i}\tilde{h}_i + \tilde{\varsigma}_{\alpha,ik}\tilde{h}_i\tilde{h}_k + \tilde{\xi}_{\alpha,ikl}\tilde{h}_i\tilde{h}_k\tilde{h}_l, \qquad \text{(B.6)}\\ \eta_{\alpha,i} &= u_{ki}\tilde{\eta}_{\alpha,k},\ \varsigma_{\alpha,ik} = u_{li}u_{mk}\tilde{\varsigma}_{\alpha,lm},\ \xi_{\alpha,ikl} = u_{mi}u_{nk}u_{rl}\tilde{\xi}_{\alpha,mnr}, \qquad \text{(B.7)}\end{aligned}$$

where there is a summation over the repeated indices. Then

$$\begin{aligned}\lambda^{(3)}_{ijk} =& \lambda^{(3-\text{tree})}_{ijk} + \sum_\alpha \frac{n_\alpha m_\alpha^4}{32\pi^2}\Bigg[\left(\xi_{\alpha,ijk} + \eta_{\alpha,i}\varsigma_{\alpha,jk} + \eta_{\alpha,k}\varsigma_{\alpha,ij} + \eta_{\alpha,j}\varsigma_{\alpha,ik}\right)\log\frac{m_\alpha^2}{m_{h_1}^2}\\ &+ \xi_{\alpha,ijk}\left(\frac{1}{2} - c_\alpha\right) + \left(\eta_{\alpha,i}\varsigma_{\alpha,jk} + \eta_{\alpha,k}\varsigma_{\alpha,ij} + \eta_{\alpha,j}\varsigma_{\alpha,ik}\right)\left(\frac{3}{2} - c_\alpha\right) + \eta_{\alpha,i}\eta_{\alpha,j}\eta_{\alpha,k}\Bigg]\\ &+ \log\frac{m_{h_1}^2}{\Lambda^2}\sum_\alpha \frac{n_\alpha m_\alpha^4}{32\pi^2}\left(\xi_{\alpha,ijk} + \eta_{\alpha,i}\varsigma_{\alpha,jk} + \eta_{\alpha,k}\varsigma_{\alpha,ij} + \eta_{\alpha,j}\varsigma_{\alpha,ik}\right), \qquad \text{(B.8)}\end{aligned}$$

where the scale dependance is isolated in the last line. This scale dependance can be eliminated in favor of measurable quantities such as CP-even scalar eigenmasses. In order to do so, let us take the general form of the scalar effective potential (B.1). Then, the tadpole gives

$$\mu_k^2 = \frac{\lambda_k}{6}v_k^2 + \sum_l \frac{\omega_{kl}+\omega_{lk}}{2}v_l^2 + \sum_\alpha \frac{n_\alpha\tilde{\eta}_{\alpha,k}m_\alpha^4}{32\pi^2 v_k}\left(\log\frac{m_\alpha^2}{m_{h_1}^2} - c_\alpha + \frac{1}{2}\right) + \log\frac{m_{h_1}^2}{\Lambda^2}\sum_\alpha\frac{n_\alpha\tilde{\eta}_{\alpha,k}m_\alpha^4}{32\pi^2 v_k}, \qquad \text{(B.9)}$$

and the summation of all CP-even scalar masses taking into account the tadpole conditions (B.9) are given by

$$\begin{aligned}\sum_k m_{h_k}^2 =& \sum_k \frac{\lambda_k}{3}v_k^2 + \frac{1}{32\pi^2}\sum_{\alpha,k} n_\alpha m_\alpha^4\left(\tilde{\eta}_{\alpha,k}^2 + \tilde{\varsigma}_{\alpha,kk} - \frac{\tilde{\eta}_{\alpha,k}}{v_k}\right)\log\frac{m_\alpha^2}{m_{h_1}^2}\\ &+ \frac{1}{32\pi^2}\sum_{\alpha,k} n_\alpha m_\alpha^4\left(\tilde{\eta}_{\alpha,k}^2\left(-c_\alpha + \frac{3}{2}\right) + \left(\tilde{\varsigma}_{\alpha,kk} - \frac{\tilde{\eta}_{\alpha,k}}{v_k}\right)\left(-c_\alpha + \frac{1}{2}\right)\right)\\ &+ \frac{1}{32\pi^2}\log\frac{m_{h_1}^2}{\Lambda^2}\sum_{\alpha,k} n_\alpha m_\alpha^4\left(\tilde{\eta}_{\alpha,k}^2 + \tilde{\varsigma}_{\alpha,kk} - \frac{\tilde{\eta}_{\alpha,k}}{v_k}\right). \qquad \text{(B.10)}\end{aligned}$$

By using (B.10), the scale dependance in (B.8) can be removed straightforward. In the $\overline{DR}$ scheme ($c_\alpha = 3/2$), the Higgs triple couplings can be written as

$$\begin{aligned}\lambda^{(3)}_{ijl} =& \lambda^{(3-\text{tree})}_{ijl} + \sum_\alpha \frac{n_\alpha m_\alpha^4}{32\pi^2}\Bigg[\left(\xi_{\alpha,ijk} + \eta_{\alpha,i}\varsigma_{\alpha,jk} + \eta_{\alpha,j}\varsigma_{\alpha,ik} + \eta_{\alpha,k}\varsigma_{\alpha,ij}\right)\log\frac{m_\alpha^2}{m_{h_1}^2}\\ &+ \eta_{\alpha,i}\eta_{\alpha,j}\eta_{\alpha,k} + \eta_{\alpha,i}\varsigma_{\alpha,jk} + \eta_{\alpha,j}\varsigma_{\alpha,ik} + \eta_{\alpha,k}\varsigma_{\alpha,it}\Bigg]\\ &+ \frac{A}{C}\sum_\alpha n_\alpha m_\alpha^4\left(\xi_{\alpha,ijk} + \eta_{\alpha,i}\varsigma_{\alpha,jk} + \eta_{\alpha,k}\varsigma_{\alpha,ij} + \eta_{\alpha,j}\varsigma_{\alpha,ik}\right), \qquad \text{(B.11)}\end{aligned}$$

JHEP02(2014)042

$$
\begin{aligned}
A =& \sum_k (m_{h_k}^2 - \frac{\lambda_k}{3} v_k^2) - \sum_{\alpha,k} \frac{n_\alpha \tilde{\eta}_{\alpha,k}^2 m_\alpha^4}{32\pi^2} - \sum_{\alpha,k} \frac{n_\alpha m_\alpha^4 \left(\tilde{\eta}_{\alpha,k}^2 + \tilde{\varsigma}_{\alpha,kk} - \frac{\tilde{\eta}_{\alpha,k}}{v_k}\right)}{32\pi^2} \log \frac{m_\alpha^2}{m_{h_1}^2} \\
C =& \sum_{\alpha,k} n_\alpha m_\alpha^4 \left(\tilde{\eta}_{\alpha,k}^2 + \tilde{\varsigma}_{\alpha,kk} - \frac{\tilde{\eta}_{\alpha,k}}{v_k}\right).
\end{aligned} \tag{B.12}
$$

In our model, we have $u_{11} = u_{22} = c$ and $u_{12} = -u_{21} = s$. Then, the coefficients in (B.6) for gauge bosons, top quark and S_0 scalar are

$$
\begin{aligned}
&\tilde{\eta}_{W,1} = \tilde{\eta}_{Z,1} = \tilde{\eta}_{t,1} = \frac{2}{v}, && \tilde{\eta}_{S_0,1} = \frac{\lambda_0 v}{m_0^2}, && \tilde{\eta}_{S_0,2} = \frac{\eta_{01} v_1}{m_0^2}. \\
&\tilde{\varsigma}_{W,11} = \tilde{\varsigma}_{Z,11} = \tilde{\varsigma}_{t,11} = \frac{2}{v^2}, && \tilde{\varsigma}_{S_0,11} = \frac{\lambda_0}{m_0^2}, && \tilde{\varsigma}_{S_0,22} = \frac{\eta_{01}}{m_0^2},
\end{aligned} \tag{B.13}
$$

and all other parameters are vanishing. For the two CP-even scalars $h_{1,2}$, we have

$$
\begin{aligned}
\tilde{\eta}_{(1,2),1} &= \{\lambda + \lambda_1 \mp [(\lambda - \lambda_1)(a-b) + 8\lambda_1^2 v_1^2]/[2\left(m_2^2 - m_1^2\right)]\} v/m_{1,2}^2, \\
\tilde{\eta}_{(1,2),2} &= \{\eta_1 + \lambda_1 \mp [(\lambda_1 - \eta_1)(a-b) + 8\lambda_1^2 v^2]/[2\left(m_2^2 - m_1^2\right)]\} v_1/m_{1,2}^2,
\end{aligned} \tag{B.14}
$$

with

$$
a = -\mu^2 + \lambda v^2/2 + \lambda_1 v_1^2/2, \; b = -\mu_1^2 + \lambda_1 v^2/2 + \eta_1 v_1^2/2. \tag{B.15}
$$

While

$$
\begin{aligned}
\tilde{\varsigma}_{(1,2),11} =& \{\lambda + \lambda_1 \mp [(\lambda - \lambda_1)(a-b) + (\lambda - \lambda_1)^2 v^2 + 8\lambda_1^2 v_1^2]/[2\left(m_2^2 - m_1^2\right)] \pm \\
& [\left((\lambda - \lambda_1)(a-b) v + 8\lambda_1^2 v v_1^2\right)^2]/[4\left(m_2^2 - m_1^2\right)^3]\}/m_{1,2}^2, \\
\tilde{\varsigma}_{(1,2),12} =& \mp [\left(15\lambda_1^2 + \lambda\lambda_1 - \lambda\eta_1 + \lambda_1\eta_1\right) v v_1]/[2m_{1,2}^2\left(m_2^2 - m_1^2\right)] \pm [((\lambda - \lambda_1)(a-b) v \\
& + 8\lambda_1^2 v v_1^2)\left((\lambda_1 - \eta_1) v_1 (a-b) + 8\lambda_1^2 v^2 v_1\right)]/[2m_{1,2}^2\left(m_2^2 - m_1^2\right)^3], \\
\tilde{\varsigma}_{(1,2),22} =& \{\eta_1 + \lambda_1 \mp [(\lambda_1 - \eta_1)(a-b) + (\lambda_1 - \eta_1)^2 v_1^2 + 8\lambda_1^2 v^2]/[2\left(m_2^2 - m_1^2\right)] \pm \\
& [\left((\lambda_1 - \eta_1)(a-b) v_1 + 8\lambda_1^2 v^2 v_1\right)^2]/[4\left(m_2^2 - m_1^2\right)^3]\}/m_{1,2}^2,
\end{aligned} \tag{B.16}
$$

and

$$
\begin{aligned}
\tilde{\xi}_{(1,2),111} =& \mp 3\{(\lambda - \lambda_1)^2 v - [\left((\lambda - \lambda_1)(a-b) v + 8\lambda_1^2 v v_1^2\right)((\lambda - \lambda_1)(a-b) + (\lambda - \lambda_1)^2 v^2 \\
& + 8\lambda_1^2 v_1^2)]/[2\left(m_2^2 - m_1^2\right)^2] + [\left((\lambda - \lambda_1)(a-b) v + 8\lambda_1^2 v v_1^2\right)^3]/[4\left(m_2^2 - m_1^2\right)^4]\} \\
& /\{2m_{1,2}^2\left(m_2^2 - m_1^2\right)\}, \\
\tilde{\xi}_{(1,2),112} =& \mp \{\left(15\lambda_1^2 + \lambda\lambda_1 - \lambda\eta_1 + \lambda_1\eta_1\right) v_1 - [\left((\lambda_1 - \eta_1)(a-b) v_1 + 8\lambda_1^2 v^2 v_1\right) \times \\
& \left((\lambda - \lambda_1)(a-b) + (\lambda - \lambda_1)^2 v^2 + 8\lambda_1^2 v_1^2\right) + 2((\lambda - \lambda_1)(\lambda_1 - \eta_1) v v_1 \\
& + 16\lambda_1^2 v v_1)\left((\lambda - \lambda_1)(a-b) v + 8\lambda_1^2 v v_1^2\right)]/[2\left(m_2^2 - m_1^2\right)^2] + \\
& [3((\lambda_1 - \eta_1)(a-b) v_1 + 8\lambda_1^2 v^2 v_1)\left((\lambda - \lambda_1)(a-b) v + 8\lambda_1^2 v v_1^2\right)^2] \\
& /[4\left(m_2^2 - m_1^2\right)^4]\}/\{2m_{1,2}^2\left(m_2^2 - m_1^2\right)\},
\end{aligned}
$$

JHEP02(2014)042

$$
\begin{aligned}
\tilde{\xi}_{(1,2),122} = &\mp \{\left(15\lambda_1^2 + \lambda\lambda_1 - \lambda\eta_1 + \lambda_1\eta_1\right) v - [\left((\lambda - \lambda_1)\,(a-b)\,v + 8\lambda_1^2 v v_1^2\right) \times \\
&\left((\lambda_1 - \eta_1)\,(a-b) + (\lambda_1 - \eta_1)^2 v_1^2 + 8\lambda_1^2 v^2\right) + 2((\lambda - \lambda_1)(\lambda_1 - \eta_1) v v_1 \\
&+ 16\lambda_1^2 v v_1)\left((\lambda_1 - \eta_1)\,(a-b)\,v_1 + 8\lambda_1^2 v^2 v_1\right)]/[2\left(m_2^2 - m_1^2\right)^2] \\
&+ [3\left((\lambda - \lambda_1)\,(a-b)\,v + 8\lambda_1^2 v v_1^2\right)\left((\lambda_1 - \eta_1)\,(a-b)\,v_1 + 8\lambda_1^2 v^2 v_1\right)^2] \\
&/[4\left(m_2^2 - m_1^2\right)^4]\}/\{2m_{1,2}^2\left(m_2^2 - m_1^2\right)\}, \\
\tilde{\xi}_{(1,2),222} = &\mp 3\{(\lambda_1 - \eta_1)^2 v_1 - [\left((\lambda_1 - \eta_1)\,(a-b)\,v_1 + 8\lambda_1^2 v^2 v_1\right)\left((\lambda_1 - \eta_1)\,(a-b)\right. \\
&\left. + (\lambda_1 - \eta_1)^2 v_1^2 + 8\lambda_1^2 v^2)\right]/[2\left(m_2^2 - m_1^2\right)^2] + [\left((\lambda_1 - \eta_1)\,(a-b)\,v_1 + 8\lambda_1^2 v^2 v_1\right)^2] \\
&/[4\left(m_2^2 - m_1^2\right)^4]\}/\{2m_{1,2}^2\left(m_2^2 - m_1^2\right)\}. \qquad \text{(B.17)}
\end{aligned}
$$

References

[1] ATLAS collaboration, *Observation of a new particle in the search for the Standard Model Higgs boson with the ATLAS detector at the LHC*, *Phys. Lett.* **B 716** (2012) 1 [arXiv:1207.7214] [INSPIRE].

[2] CMS collaboration, *Observation of a new boson at a mass of 125 GeV with the CMS experiment at the LHC*, *Phys. Lett.* **B 716** (2012) 30 [arXiv:1207.7235] [INSPIRE].

[3] ATLAS collaboration, *Measurements of Higgs boson production and couplings in diboson final states with the ATLAS detector at the LHC*, *Phys. Lett.* **B 726** (2013) 88 [arXiv:1307.1427] [INSPIRE].

[4] ATLAS collaboration, *Combined coupling measurements of the Higgs-like boson with the ATLAS detector using up to 25 fb^{-1} of proton-proton collision data*, ATLAS-CONF-2013-034 (2013).

[5] ATLAS collaboration, *Combined measurements of the mass and signal strength of the Higgs-like boson with the ATLAS detector using up to 25 fb^{-1} of proton-proton collision data*, ATLAS-CONF-2013-014 (2013).

[6] CMS collaboration, *Combination of standard model Higgs boson searches and measurements of the properties of the new boson with a mass near 125 GeV*, CMS-PAS-HIG-13-005 (2013).

[7] Tevatron New Physics Higgs Working Group, CDF and D0 collaboration, *Updated Combination of CDF and D0 Searches for Standard Model Higgs Boson Production with up to 10.0 fb^{-1} of Data*, arXiv:1207.0449 [INSPIRE].

[8] ATLAS collaboration, *Measurements of the properties of the Higgs-like boson in the two photon decay channel with the ATLAS detector using 25* fb^{-1} *of proton-proton collision data*, ATLAS-CONF-2013-012 (2013).

[9] CMS collaboration, *Updated measurements of the Higgs boson at 125 GeV in the two photon decay channel*, CMS-PAS-HIG-13-001 (2013).

JHEP02(2014)042

[10] ATLAS collaboration, *Evidence for the spin-0 nature of the Higgs boson using ATLAS data*, *Phys. Lett.* **B 726** (2013) 120 [arXiv:1307.1432] [INSPIRE].

[11] ATLAS collaboration, *Study of the spin of the new boson with up to 25 fb^{-1} of ATLAS data*, ATLAS-CONF-2013-040 (2013).

[12] CMS collaboration, *Study of the Mass and Spin-Parity of the Higgs Boson Candidate Via Its Decays to Z Boson Pairs*, *Phys. Rev. Lett.* **110** (2013) 081803 [arXiv:1212.6639] [INSPIRE].

[13] CMS collaboration, *Properties of the Higgs-like boson in the decay H to ZZ to 4l in pp collisions at $\sqrt{s} = 7$ and 8 TeV*, CMS-PAS-HIG-13-002 (2013).

[14] LHC/LC Study Group collaboration, G. Weiglein et al., *Physics interplay of the LHC and the ILC*, *Phys. Rept.* **426** (2006) 47 [hep-ph/0410364] [INSPIRE].

[15] M.E. Peskin, *Comparison of LHC and ILC Capabilities for Higgs Boson Coupling Measurements*, arXiv:1207.2516 [INSPIRE].

[16] A. Abada, D. Ghaffor and S. Nasri, *A Two-Singlet Model for Light Cold Dark Matter*, *Phys. Rev.* **D 83** (2011) 095021 [arXiv:1101.0365] [INSPIRE].

[17] A. Abada and S. Nasri, *Phenomenology of a Light Cold Dark Matter Two-Singlet Model*, *Phys. Rev.* **D 85** (2012) 075009 [arXiv:1201.1413] [INSPIRE].

[18] A. Abada and S. Nasri, *RGE of a Cold Dark Matter Two-Singlet Model*, *Phys. Rev.* **D 88** (2013) 016006 [arXiv:1304.3917] [INSPIRE].

[19] A. Ahriche and S. Nasri, *Light Dark Matter, Light Higgs and the Electroweak Phase Transition*, *Phys. Rev.* **D 85** (2012) 093007 [arXiv:1201.4614] [INSPIRE].

[20] K. Cheung, J.S. Lee and P.-Y. Tseng, *Higgs Precision (Higgcision) Era begins*, *JHEP* **05** (2013) 134 [arXiv:1302.3794] [INSPIRE].

[21] G. Bélanger, B. Dumont, U. Ellwanger, J. Gunion and S. Kraml, *Status of invisible Higgs decays*, *Phys. Lett.* **B 723** (2013) 340 [arXiv:1302.5694] [INSPIRE].

[22] J.R. Espinosa, M. Muhlleitner, C. Grojean and M. Trott, *Probing for Invisible Higgs Decays with Global Fits*, *JHEP* **09** (2012) 126 [arXiv:1205.6790] [INSPIRE].

[23] O. Lebedev, H.M. Lee and Y. Mambrini, *Vector Higgs-portal dark matter and the invisible Higgs*, *Phys. Lett.* **B 707** (2012) 570 [arXiv:1111.4482] [INSPIRE].

[24] C. Englert, M. Spannowsky and C. Wymant, *Partially (in)visible Higgs decays at the LHC*, *Phys. Lett.* **B 718** (2012) 538 [arXiv:1209.0494] [INSPIRE].

[25] G. Bélanger, B. Dumont, U. Ellwanger, J. Gunion and S. Kraml, *Global fit to Higgs signal strengths and couplings and implications for extended Higgs sectors*, *Phys. Rev.* **D 88** (2013) 075008 [arXiv:1306.2941] [INSPIRE].

[26] P.P. Giardino, K. Kannike, I. Masina, M. Raidal and A. Strumia, *The universal Higgs fit*, arXiv:1303.3570 [INSPIRE].

[27] CMS collaboration, *Search for invisible Higgs produced in association with a Z boson*, (2013).

[28] CMS collaboration, *Search for an Invisible Higgs Boson*, CMS-PAS-HIG-13-013 (2013).

[29] CDMS collaboration, Z. Ahmed et al., *Search for Weakly Interacting Massive Particles with the First Five-Tower Data from the Cryogenic Dark Matter Search at the Soudan Underground Laboratory*, *Phys. Rev. Lett.* **102** (2009) 011301 [arXiv:0802.3530] [INSPIRE].

JHEP02(2014)042

[30] CDMS-II collaboration, Z. Ahmed et al., *Dark Matter Search Results from the CDMS II Experiment*, *Science* **327** (2010) 1619 [arXiv:0912.3592] [INSPIRE].

[31] XENON collaboration, J. Angle et al., *First Results from the XENON10 Dark Matter Experiment at the Gran Sasso National Laboratory*, *Phys. Rev. Lett.* **100** (2008) 021303 [arXiv:0706.0039] [INSPIRE].

[32] XENON100 collaboration, E. Aprile et al., *First Dark Matter Results from the XENON100 Experiment*, *Phys. Rev. Lett.* **105** (2010) 131302 [arXiv:1005.0380] [INSPIRE].

[33] OPAL collaboration, G. Abbiendi et al., *Decay mode independent searches for new scalar bosons with the OPAL detector at LEP*, *Eur. Phys. J.* **C 27** (2003) 311 [hep-ex/0206022] [INSPIRE].

[34] E.W. Kolb and M.S. Turner, *The Early Universe*, Addison-Wesley, New York U.S.A. (1988), pg. 719.

[35] S. Weinberg, *Cosmology*, Oxford University Press, Oxford U.K. (2008), pg. 544.

[36] PLANCK collaboration, P. Ade et al., *Planck 2013 results. I. Overview of products and scientific results*, arXiv:1303.5062 [INSPIRE].

[37] COGENT collaboration, C. Aalseth et al., *Results from a Search for Light-Mass Dark Matter with a P-type Point Contact Germanium Detector*, *Phys. Rev. Lett.* **106** (2011) 131301 [arXiv:1002.4703] [INSPIRE].

[38] M.A. Shifman, A. Vainshtein and V.I. Zakharov, *Remarks on Higgs Boson Interactions with Nucleons*, *Phys. Lett.* **B 78** (1978) 443 [INSPIRE].

[39] H.-Y. Cheng, *Low-energy Interactions of Scalar and Pseudoscalar Higgs Bosons With Baryons*, *Phys. Lett.* **B 219** (1989) 347 [INSPIRE].

[40] J. Gasser, H. Leutwyler and M. Sainio, *Sigma term update*, *Phys. Lett.* **B 253** (1991) 252 [INSPIRE].

[41] QCDSF collaboration, G.S. Bali et al., *The strange and light quark contributions to the nucleon mass from Lattice QCD*, *Phys. Rev.* **D 85** (2012) 054502 [arXiv:1111.1600] [INSPIRE].

[42] S. Dürr et al., *Sigma term and strangeness content of octet baryons*, *Phys. Rev.* **D 85** (2012) 014509 [arXiv:1109.4265] [INSPIRE].

[43] LUX collaboration, D. Akerib et al., *First results from the LUX dark matter experiment at the Sanford Underground Research Facility*, arXiv:1310.8214 [INSPIRE].

[44] E.N. Glover and J. van der Bij, *Higgs boson pair production via gluon fusion*, *Nucl. Phys.* **B 309** (1988) 282 [INSPIRE].

[45] T. Plehn, M. Spira and P. Zerwas, *Pair production of neutral Higgs particles in gluon-gluon collisions*, *Nucl. Phys.* **B 479** (1996) 46 [*Erratum ibid.* **B 531** (1998) 655] [hep-ph/9603205] [INSPIRE].

[46] U. Baur, T. Plehn and D.L. Rainwater, *Measuring the Higgs boson self coupling at the LHC and finite top mass matrix elements*, *Phys. Rev. Lett.* **89** (2002) 151801 [hep-ph/0206024] [INSPIRE].

[47] U. Baur, T. Plehn and D.L. Rainwater, *Determining the Higgs boson selfcoupling at hadron colliders*, *Phys. Rev.* **D 67** (2003) 033003 [hep-ph/0211224] [INSPIRE].

JHEP02(2014)042

[48] J. Baglio et al., *The measurement of the Higgs self-coupling at the LHC: theoretical status*, *JHEP* **04** (2013) 151 [arXiv:1212.5581] [INSPIRE].

[49] U. Baur, T. Plehn and D.L. Rainwater, *Probing the Higgs selfcoupling at hadron colliders using rare decays*, *Phys. Rev.* **D 69** (2004) 053004 [hep-ph/0310056] [INSPIRE].

[50] M.J. Dolan, C. Englert and M. Spannowsky, *Higgs self-coupling measurements at the LHC*, *JHEP* **10** (2012) 112 [arXiv:1206.5001] [INSPIRE].

[51] S. Kanemura, Y. Okada, E. Senaha and C.-P. Yuan, *Higgs coupling constants as a probe of new physics*, *Phys. Rev.* **D 70** (2004) 115002 [hep-ph/0408364] [INSPIRE].

[52] A. Arhrib, R. Benbrik, C.-H. Chen, R. Guedes and R. Santos, *Double Neutral Higgs production in the Two-Higgs doublet model at the LHC*, *JHEP* **08** (2009) 035 [arXiv:0906.0387] [INSPIRE].

[53] M. Moretti, S. Moretti, F. Piccinini, R. Pittau and J. Rathsman, *Production of Light Higgs Pairs in 2-Higgs Doublet Models via the Higgs-strahlung Process at the LHC*, *JHEP* **11** (2010) 097 [arXiv:1008.0820] [INSPIRE].

[54] E. Asakawa, D. Harada, S. Kanemura, Y. Okada and K. Tsumura, *Higgs boson pair production in new physics models at hadron, lepton and photon colliders*, *Phys. Rev.* **D 82** (2010) 115002 [arXiv:1009.4670] [INSPIRE].

[55] M.J. Dolan, C. Englert and M. Spannowsky, *New Physics in LHC Higgs boson pair production*, *Phys. Rev.* **D 87** (2013) 055002 [arXiv:1210.8166] [INSPIRE].

[56] U. Ellwanger, *Higgs pair production in the NMSSM at the LHC*, *JHEP* **08** (2013) 077 [arXiv:1306.5541] [INSPIRE].

[57] J. Cao, Z. Heng, L. Shang, P. Wan and J.M. Yang, *Pair Production of a 125 GeV Higgs Boson in MSSM and NMSSM at the LHC*, *JHEP* **04** (2013) 134 [arXiv:1301.6437] [INSPIRE].

[58] S. Dawson, S. Dittmaier and M. Spira, *Neutral Higgs boson pair production at hadron colliders: QCD corrections*, *Phys. Rev.* **D 58** (1998) 115012 [hep-ph/9805244] [INSPIRE].

JHEP02(2014)042